Chromatography **2022**, *43,* 1-14

Focusing Review

Development of Novel Analysis and Characterization Methods Utilizing Reaction Dynamics in a Separation Capillary

Toshio TAKAYANAGI*

Graduate School of Technology, Industrial and Social Sciences, Tokushima University, 2-1 Minamijyousanjima-cho, Tokushima 770-7506, Japan

Abstract

Electrophoretic migration of an analyte in capillary electrophoresis (CE) reflects reaction dynamics of the analyte in solution. In affinity CE, an analyte of interest interacts with a modifier added in the separation buffer in fast equilibrium, and effective electrophoretic mobility of the analyte is contributed from its equilibrium species. Precise measurement of effective electrophoretic mobility allows analyzing the equilibrium. Analysis of equilibria under CE separation possesses several advantages against traditional analyses in homogeneous solution; coexisting substances including impurities and kinetically generated substances are resolved by CE from the equilibrium species of interest. Characteristics of the CE analysis have been applied to analyses of acid-base equilibria of degradable substances and ion-association equilibria in an aqueous solution. Since CE is operated in an open-tubular capillary, it is also suitable for the characterization of carbon nanoclusters such as graphene and carbon nanotube, and measurement of effective electrophoretic mobility helps characterization of nanoclusters. A novel analysis technique of capillary electrophoresis/dynamic frontal analysis (CE/DFA) has also been proposed for the analysis of such reactions as involving equilibria and kinetic reactions. In CE/DFA, kinetically generated product is continuously resolved from the equilibrium species, and a plateau signal would be detected when the reaction rate is constant. Michaelis-Menten constants have successfully been determined through the plateau height by CE/DFA. In this review, analysis and characterization methods utilizing reaction dynamics in a separation capillary are summarized.

Keywords: Capillary electrophoresis; Degradable substances; Ion-association equilibria; Carbon nanoclusters; Enzyme assay

1. Introduction

Capillary electrophoresis (CE) is a versatile separation and analysis system for ionic substances. Analyte ion of interest electrophoretically migrates toward the opposite electrode in a separation buffer, and ionic substances are resolved by the difference in their inherent electrophoretic mobility. When the separation among target analytes is not sufficient, affinity reagents are often used to control the electrophoretic mobility of the analytes and to improve the separation efficiency among the analytes. The separation development is essentially based on the dynamic equilibrium in a separation capillary; the analytes in the sample solution would interact with the affinity reagent in equilibrium during the electrophoresis, and effective electrophoretic mobility of the analyte would change by the interaction. Analytes of interest can be resolved by the different degree of the affinity interaction. Since the effective electrophoretic mobility of an analyte changes with the degree of the interaction, we can analyze the affinity interaction or the dynamic equilibrium by measuring the changes in effective electrophoretic mobility.

Chemical equilibria are traditionally analyzed in a homogeneous solution, such as potentiometric and spectrophotometric titrations. These analysis methods are simple and well-established, but unavoidable disadvantages exist. A pure analyte should be prepared for the titration and equilibrium should be maintained in a homogeneous solution. On the other hand, these restrictions can be tolerated in the CE analysis [1-3]. In the analysis of dynamic equilibria by CE, the measurement is the migration

*Corresponding author: Toshio TAKAYANAGI
Tel: +81-88-656-7409; Fax: +81-88-656-7409
E-mail: Toshio.takayanagi@tokushima-u.ac.jp

Received: 1 December 2021
Accepted: 10 January 2022
J-STAGE Advance Published: 20 January 2022
DOI: 10.15583/jpchrom.2021.022

time from the injection point to the detection point, since the equilibrium in a separation capillary results in the effective electrophoretic mobility of an analyte. Coexisting substances including impurities are tolerated in the CE analysis, since they are electrophoretically resolved from the target analyte. The separation characteristic would affirmatively be utilized for such substances as are not stable and easily degradable. As far as the residual species of an analyte can be detected, the effective electrophoretic mobility of the analyte is measured and the equilibrium of interest would be analyzed with the CE signal.

The CE separation would also be utilized for the substances with kinetic phenomena. When a substance includes any kinetic phenomena, the amount and/or the concentration of the substance changes during the electrophoretic migration in a separation capillary. When the generated substance is detected, the signal profile reflects the progress of the kinetic reaction.

This review introduces some cases of analysis and characterization utilizing reaction dynamics in a separation capillary.

2. Analysis of acid-base equilibria of degradable substances

2.1. Analysis of acid-base equilibrium through changes in effective electrophoretic mobility

Acid-base equilibrium is one of fundamental physicochemical equilibria in an aqueous solution, and it is a major subject analyzed by CE [3]. Equilibria of protonation or deprotonation of weak acids and bases accompany the change in the number of electric charge, and effective electrophoretic mobility of the acid or the base changes along with protonation or deprotonation. The acid-base equilibrium is defined with acid dissociation constant. For example, an acid dissociation equilibrium of a monoprotic acid, HA, is expressed as in equilibrium (1) with an acid dissociation constant, K_a, (2).

$$\mathrm{HA} \overset{K_a}{\rightleftharpoons} \mathrm{H^+} + \mathrm{A^-} \qquad (1)$$

$$K_a = \frac{[\mathrm{H^+}][\mathrm{A^-}]}{[\mathrm{HA}]} \qquad (2)$$

When the equilibrium between two species of HA and A^- is sufficiently fast against the separation time in CE, only single peak would be detected with its effective electrophoretic mobility. The effective electrophoretic mobility of the acid, μ_{ep}', is expressed as in Eq. (3) including an acid dissociation constant.

$$\mu_{ep}' = \frac{[\mathrm{H^+}]\,\mu_{HA}}{[\mathrm{H^+}] + K_a} + \frac{K_a\,\mu_A}{[\mathrm{H^+}] + K_a} \qquad (3)$$

In Eq. (3), μ_{HA} and μ_A are the electrophoretic mobility of HA and A^- species, respectively. The acid-base equilibrium accompanies the dissociation of a charged H^+. In this case of HA, the effective electrophoretic mobility of the acid changes from zero (μ_{HA}) to a negative value (μ_A). Since the effective electrophoretic mobility of the acid changes with pH, H^+ can be considered as an affinity reagent and CE separation under pH control would be classified as one of affinity CE (ACE). Anyway, drastic change in the effective electrophoretic mobility would be observed with an acid HA over the pH range around its pK_a value. Conversely, pK_a values can be determined through the measurement and the analysis of the effective electrophoretic mobility. The analysis is also applicable to bases, as well as to polyprotic acids and bases [3].

2.2. Detection of equilibrium species and its equilibrium analysis by CE under concomitant with kinetic reaction

A single peak would be detected for fast equilibrium species with an effective electrophoretic mobility of weighted average, as discussed in section 2.1. On the other hand, two equilibrium species would be identified as different substances and they are electrophoretically resolved by CE, when the equilibrium between two species is sufficiently slow. Further, an equilibrium would be shifted from the equilibrium species during CE separation, when the reaction rate is moderate. Dissociated species would continuously be generated from one of the equilibrium species, and the dissociated species would be detected as a leading/tailing signal. Such signal profiles reflect kinetic phenomena of equilibrium species, and the separation mode is named as non-equilibrium capillary electrophoresis from equilibrium mixture (NECEEM) [4-7].

In addition to the equilibrium between two species, kinetic reaction may accompany to the equilibrium, as written in reaction (4).

$$\mathrm{A_1} \overset{K}{\rightleftharpoons} \mathrm{A_2} \overset{k}{\rightarrow} \mathrm{B} \qquad (4)$$

Two species of A_1 and A_2 are in fast equilibrium, and B is kinetically formed from one of the equilibrium species; formation of B is defined as a side reaction to the main equilibrium. When the formation rate of B is sufficiently fast, species of A_1 and A_2 would not be present after the CE separation and they would not be detected. On the other hand, equilibrium species of A_1 and A_2 would be detected even in the concomitant with the kinetic reaction, when the formation rate of B is tolerably slow and equilibrium species of A_1 and/or A_2 exist at their detection time. Additionally, kinetically formed species from equilibrium species is electrophoretically resolved from the equilibrium species during electrophoresis. The kinetically formed

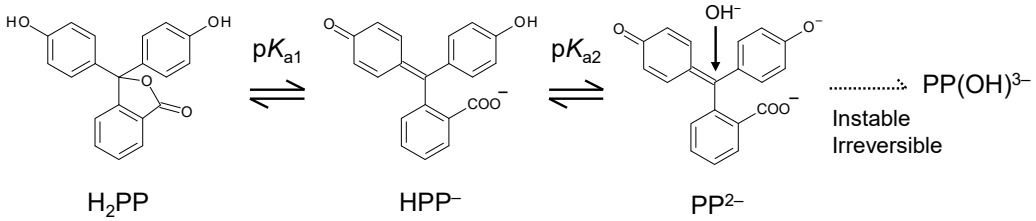

Fig. 1. Acid-base equilibria of phenolphthalein. Chemical species of H_2PP, HPP^-, and PP^{2-} are in fast equilibrium, while $PP(OH)^{3-}$ is gradually and irreversibly generated in an alkaline aqueous solution.

species would be detected as leading/tailing signal to the peak signal of the equilibrium species, because the kinetic reaction continuously proceeds during the electrophoresis. That is to say, equilibrium between A_1 and A_2 can be analyzed through its effective electrophoretic mobility even under accompanying kinetic side-reactions. Advantage on using CE for equilibrium analysis over conventional titration analyses is that such equilibrium as accompanying side-reaction can be analyzed in addition under the presence of impurities.

2.3. Determination of acid dissociation constants under degrading conditions

It is mentioned in early stage of pK_a determinations by ACE that the equilibrium analysis can be made in such solutions containing coexisting substances, *i.e.*, "highly pure and highly stable samples are unnecessary" [8]. The study suggested that degraded species from the equilibrium species generated prior to the CE analysis is resolved from the equilibrium species of interest and that the equilibrium analysis would be made by ACE with CE resolution from the coexisting degraded species. However, any practical example of degrading substance was not demonstrated.

Phenolphthalein is a well-known acid-base indicator, and it is frequently used in acid-base titrations. Acid-base equilibria of phenolphthalein is shown in Fig. 1. Red color of phenolphthalein is developed by the deprotonation of phenolic OH forming a conjugated dianion species, PP^{2-} (Fig. 1). However, phenolphthalein is a labile substance, and it degrades in an alkaline aqueous solution by the addition of OH^- to the central carbon atom. A colorless species of $PP(OH)^{3-}$ is gradually generated as shown in Fig. 1. Because of the degradation reaction forming $PP(OH)^{3-}$ species, the total concentration of the equilibrium species, $[H_2PP] + [HPP^-] + [PP^{2-}]$, decreases along with the standing time. If a considerable portion of the equilibrium species degrades, the total concentration of equilibrium species consequently decreases. Therefore, it is difficult to determine its pK_a values by spectrophotometric titration. Stopped-flow measurement of UV-vis spectra has been proposed to reduce the formation of the degraded species of phenolphthalein, and acid dissociation constants of pK_{a1} = 9.05 and pK_{a2} = 9.50 were reported [9]. However, the stopped-flow analysis could not exclude the contribution of the degraded species.

Analysis of acid dissociation equilibria by CE was firstly demonstrated with such phenolphthalein as degradable in an alkaline aqueous solution [10]. Electropherograms of phenolphthalein under several pH conditions are shown in Fig. 2 [10]. Methyl orange was used as a reference substance. The migration time of phenolphthalein got much longer at alkaline pH conditions. Phenolphthalein is more anionic at alkaline pH conditions by its acid-base equilibria, and anionic species of phenolphthalein are dominant by the deprotonation. A distinct peak of the equilibrium species is still detected at pH 11.6, although the peak height is much suppressed by the degradation. It is also noticed from the electropherogram that more anionic species, $PP(OH)^{3-}$, is continuously resolved from the equilibrium species and a tailing signal is concomitant with the peak of the equilibrium species. Changes in effective electrophoretic mobility of phenolphthalein is shown in Fig. 3. Effective electrophoretic mobility of phenolphthalein has successfully

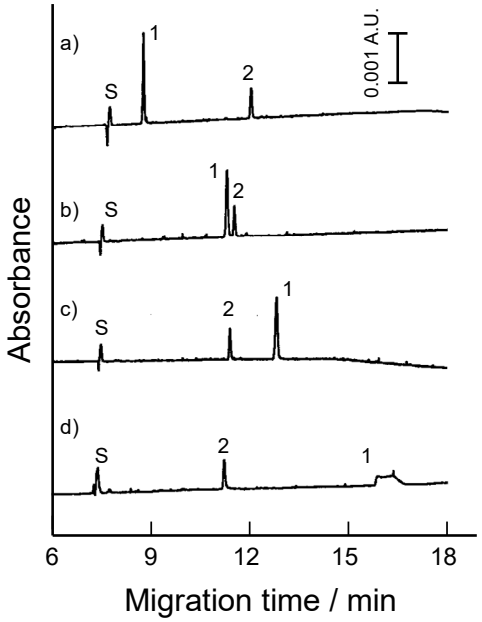

Fig. 2. Electropherograms for phenolphthalein and methyl orange at different pH conditions. pH conditions: a) 8.64; b) 9.42; c) 9.81; d) 11.60. Signals: 1, phenolphthalein; 2, methyl orange; S, ethanol (EOF marker). Rearranged from a figure in Ref. 10.

been obtained even at its degradable condition of pH 11.60. Two steps of the acid dissociation constants were successfully determined with phenolphthalein by analyzing the changes in the effective electrophoretic mobility: pK_{a1} = 8.84 and pK_{a2} = 9.40 [10].

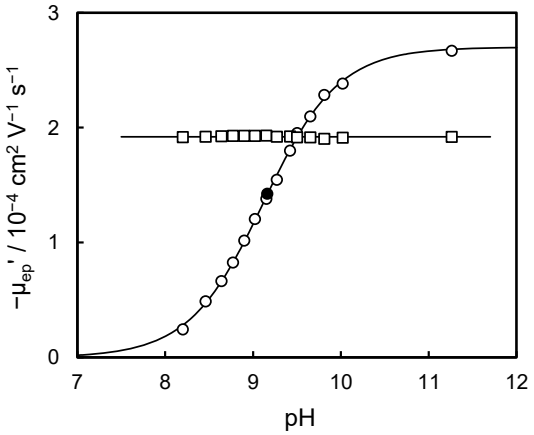

Fig. 3. Changes in the electrophoretic mobility of the reagent by the change in pH of the separation buffer. ○: freshly prepared phenolphthalein; ●: phenolphthalein measured after 24 h standing in a borate buffer solution; □: methyl orange. Solid curves show the simulation of the mobility change under acid-base equilibria. Rearranged from a figure in Ref. 10.

The prominent characteristics of CE separation on equilibrium analysis were demonstrated with labile compounds of pharmaceutical candidates [11]. p*K*a values of alkaline degradable benzenesulfonic acid phenethyloxy-phenyl esters were determined with the undegraded CE signal in the presence of the degradation products. pK_a values of six kinds of anti-inflammatory aminoindanones were successfully determined, although they are degradable at pH > 5 forming neutral indanone [12]. The decomposition of the tertiary amino derivatives was especially fast with first-order half-lives of less than 10 min observed at pH 7.4. Urinary 3-methylhistidine (3-MH) and 1-methylhistidine (1-MH) are generated by the degradation of skeletal muscle proteins, and pK_a values of the degraded species, 3-MH and 1-MH, were determined through the change in effective electrophoretic mobility; three steps of the acid dissociation reactions were analyzed by CE [13]. An herbicide of metribuzin degrades to form deaminometribuzin, deaminodiketometribuzin, and diketometribuzin. pK_a values of the four substances were also determined under the degraded conditions by the mobility change at a constant ionic strength of 0.05 [14]. Large volume sample stacking and solid-phase extraction were used to improve the detection sensitivity of the degradants. pK_a values of warfarin and its oxidative metabolites, hydroxywarfarins, were successfully determined by CE [15]. Equilibrium analysis of labile compound was also made on a phenolphthalein derivative of terabromophenolphthalein ethyl ester (TBPE) [16]. TBPE is easily degradable in acidic solutions by hydrolysis of the ester moiety, and a short capillary was used to suppress the degradation during the electrophoretic migration. Although it was difficult to detect the CE signal of TBPE at pH below 4.0 by the fast hydrolysis even with the short capillary, a pK_a value of 3.47 was determined with the change in the effective electrophoretic mobility of the detected species (Fig. 4). It has been fortunate that TBPE is a monoprotic acid and that the electrophoretic mobility of the protonated TBPE is neutral with its electrophoretic mobility to be zero. A pK_a value of a major tranquilizer, haloperidol, was also determined by the CE analysis in the presence of its degraded species of 4-(4-chlorophenyl)-4-hydroxypiperidine. A pK_a value of the degradant was also determined [17]. pK_a values of acid-degradable pravastatin [18] and hexamethylenetetramine [19] were determined under degraded conditions without any interference from the degraded species. Determination of acid dissociation constants by CE was also successful with alkaline-degradable catecholamines [20], ascorbic acid [21], and flavin derivatives [22]. Heat-degradable bupropion [23] and hydrochlorothiazide [24] were also examined.

In this way, CE analysis is applicable to the determination of equilibrium constants, even accompanying any kinetic side reaction to the fast equilibrium of interest. As far as the equilibrium species is detected as a peak

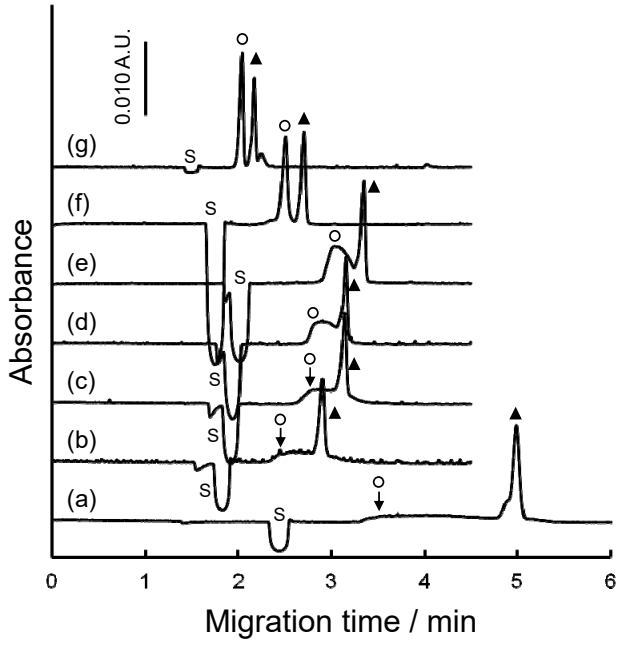

Fig. 4. Electropherograms for TBPE and phenol red at different pH conditions. Sample solution contains 2×10^{-5} M K·TBPE, 2×10^{-5} M phenol red and 1%(v/v) EtOH. pH of the separation buffer: (a) 3.97, (b) 4.32, (c) 4.51, (d) 4.90, (e) 5.04, (f) 5.58, (g) 6.09. Signals: ○, TBPE; ▲, phenol red. S: water dip of the sample solution or ethanol in the sample solution. Rearranged from a figure in Ref. 16.

signal, the equilibrium can be analyzed through the measurement of effective electrophoretic mobility even under the degradation conditions.

3. Analysis of ion-association equilibrium in an aqueous solution

3.1. Ion-association equilibria in analytical chemistry

Ion-association equilibrium between organic ions has widely been utilized in the research field of analytical chemistry by coupling it with distribution to hydrophobic media [25]. Ion-pair solvent extraction and ion-pair reversed-phase HPLC are practical ones. Ion-association equilibrium is fundamentally based on electrostatic interaction between a cation and an anion. When both cation and anion are organic ions, hydrophobic interaction also contributes to the ion-association equilibrium. Hydrophobic interaction has been interpreted by the change in the hydration of ions. Water molecules of the hydrated ion are released by the ion-association reaction between a cation and an anion. The release of water molecules contributes to the increase in entropy, as well as the decrease in Gibbs free energy. Therefore, hydrophobic ion-association reaction is promoted in an aqueous solution. Generally, organic ion-associates easily precipitate in an aqueous solution, and it was difficult to analyze the equilibrium by ordinary analysis methods [25]. Ion-pair solvent extraction could give the ion-association constant in aqueous solution, but the reliability was inferior [26].

Although ion-association reaction has been utilized by coupling it with distribution to hydrophobic media, ion-association equilibrium in an aqueous solution has not been utilized directly, until CE was thoroughly noticed. Ion-association equilibrium between a cation C^+ and an anion A^- is expressed as in reaction (5) with an ion-association constant, K_{ass}, as in Eq. (6).

$$C^+ + A^- \overset{K_{ass}}{\rightleftharpoons} C^+ \cdot A^- \qquad (5)$$

$$K_{ass} = \frac{[C^+ \cdot A^-]}{[C^+][A^-]} \qquad (6)$$

Reasons for the lack of usages are: (1) utilization method of ion-association equilibrium in a homogeneous aqueous phase was not developed and (2) ion-association equilibrium in an aqueous solution was not investigated systematically. CE possesses prominent features on both utilization and analysis of ion-association equilibrium in an aqueous solution without distribution to another phase. A homogeneous aqueous solution is introduced into an open-tubular capillary in CE separations. Although organic ion-associates are likely precipitable in an aqueous solution, the solubility of ion-associates is somewhat tolerated in CE. Because an analyte ion is under dynamic equilibrium with pairing ion in the analyte zone.

The ion-association equilibrium involves changes in the effective electrophoretic mobility of an analyte, C^+ or A^-, when an ion with opposite charge is added in the separation buffer as a pairing ion and a separation modifier. Thus, the effective charge of the analyte ion decreases by an ion-association equilibrium and the electrophoretic mobility of the analyte ion changes by forming an ion-associate (Fig. 5). To put it the other way around, ion-association equilibrium can be analyzed through the changes in the electrophoretic mobility.

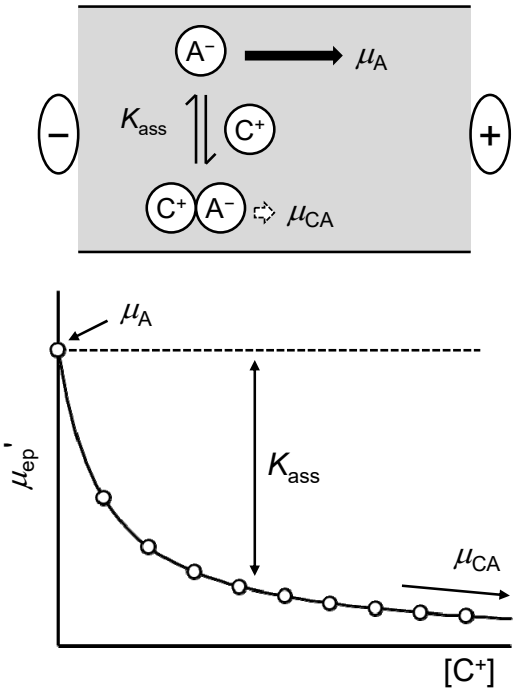

Fig. 5. Top: Schematic illustration of an ion-association equilibrium in a CE capillary. An analyte anion, A^-, interacts with a pairing cation, C^+, in the separation buffer, forming an ion-associate, $C^+ \cdot A^-$. Bottom: The effective electrophoretic mobility of A^-, μ_{ep}', decreases with increasing concentrations of C^+ by the equilibrium. The μ_{ep}' changes from its inherent electrophoretic mobility, μ_A, to that of the ion-associate, μ_{CA}.

3.2. Utilization of ion-ion interactions in CE

Nashabeh and Rassi firstly revealed the usefulness of quaternary ammonium ion as a separation modifier in CE for the separation of aminopyridine derivatized glycoproteins [27]. The usage of hydrophobic quaternary ammonium ion was interpreted as ion-association reaction on a CE separation of highly charged anionic metal chelates [28]. Anionic ion-association reagent of alkylsulfonates were used for the separation of angiotensin-converting enzyme inhibitors [29]. Applications of conventional ion-pairing reagents to the CE separation are reviewed by Shelton, *et al.* [30].

3.3. Analysis of ion-association equilibrium in an aqueous solution by CE

Ion-association equilibrium is generally in fast reversible reaction, and effective electrophoretic mobility of an ion is contributed from both species of the free ion and the ion-associate as a value of weighted average. Practically, an analyte anion A^- is assumed to form an ion-associate with a pairing cation C^+. The effective electrophoretic mobility of an analyte anion, μ_{ep}', is contributed from free A^- and ion-associate $C^+ \cdot A^-$, as written in Eq. (7).

$$\mu_{ep}' = \frac{\mu_A}{[A^-] + [C^+ \cdot A^-]} + \frac{[C^+ \cdot A^-]\ \mu_{CA}}{[A^-] + [C^+ \cdot A^-]} \qquad (7)$$

In Eq. (7), μ_A and μ_{CA} are the electrophoretic mobility of A^- and $C^+ \cdot A^-$, respectively. Equation (7) is converted to Eq. (8) by coupling with the ion-association constant.

$$\mu_{ep}' = \frac{\mu_A}{1 + [C^+]\ K_{ass}} + \frac{[C^+]\ K_a\ \mu_{CA}}{1 + [C^+]\ K_{ass}} \qquad (8)$$

Equation (8) suggests that a value of μ_{ep}' changes with increasing concentrations of C^+. Ion-association constant, K_{ass}, can be determined by fitting the results of μ_{ep}' to Eq. (8) [1,2].

3.4. Factors contributing to ion-associability in an aqueous solution

Clarification of structure-property relationship is essential to design and to control the separation system, and factors contributing to the ion-associability in an aqueous solution are examined by comparing ion-association constants.

Ion-associability of several aromatic anions was examined with a series of quaternary ammonium ions. Symmetrical quaternary ammonium ions with different molecular size were used to evaluate the contribution of hydrophobicity [31,32]. Ion-association constants of the aromatic anions, K_{ass}, were determined by the CE analysis. Logarithmic values of K_{ass} were plotted against the carbon number of the quaternary ammonium ions to examine a linear free energy relationship (Fig. 6) [32]. The K_{ass} values of each anion increased with increasing size/volume of the pairing cation, and a linear relationship was obtained with the K_{ass} values. The result suggests that hydrophobic cations are more associable with the aromatic anions. The average slope of 0.06 suggests that ion-association constant increases by $10^{0.06}$ with increasing number of a methylene moiety [32]. The number of methylene moiety is related with the degree of the hydrophobicity of the quaternary ammonium ions, and the value of $10^{0.06}$ is interpreted as the contribution of the hydrophobicity as one methylene group in an aqueous solution. It is reported that the contribution of methylene group to the ion-associability is about $10^{0.6}$ in liquid-liquid distribution system [25]. Therefore, the contribution of hydrophobicity in an aqueous solution is about 1/10 of the liquid-liquid distribution system. Contribution of the hydrophobicity to the ion-association constants was also examined with anionic azo dyes [33] and anionic methyl orange analogues [34].

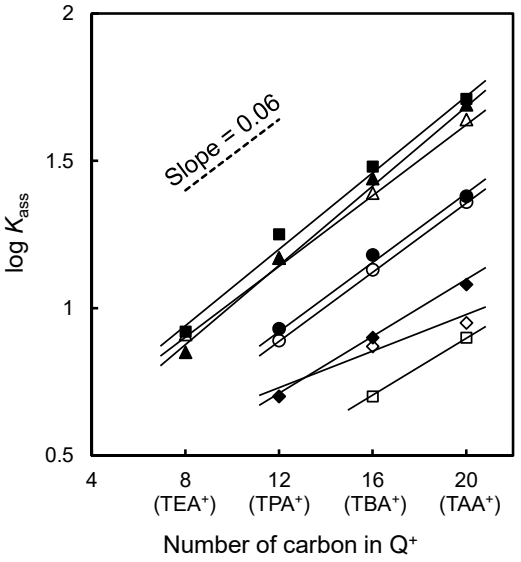

Fig. 6. Relationships between ion-association constants and the carbon number of quaternary ammonium ions (Q^+). Rearranged from a figure in Ref. 32.

Ion-association equilibrium was also examined based on the electrostatic interactions. Rasmussen and Bjerrum determined ion-association constants between cationic cobalt(III) complexes and inorganic anions [35]. Both values of K and K^o are mentioned; they are directly determined by CE. Equilibrium constants of K were corrected as thermodynamic K^o values with the ionic strength of the separation buffer. It is noted in the K values that such ion-associate as formed between highly charged ions gave larger ion-association constant: $[Co(en)_2Cl_2]^+ - ClO_4^-$ (7 M^{-1}) < $[Co(NH_3)_5Cl]^{2+} - ClO_4^-$ (9 M^{-1}) < $[Co(NH_3)_5Cl]^{2+} - SO_4^{2-}$ (136 M^{-1}). The order agrees with the concept of the electrostatic interaction. Electrostatic interaction was also investigated with primary to quaternary ammonium ions from its ion-associability with some aromatic anions [36]. Minimum ion-association constants of the aromatic anions were obtained with the secondary ammonium ions, $HxMA^+$. The tendency informs that the ion-associability changes from electrostatic (primary) to hydrophobic (quaternary) [36].

Recognition of the intramolecular distance between two ionic sites in a molecule was examined. Divalent quaternary ammonium ions were designed to utilize the multipoint interactions [37]. Distance between two cationic groups was controlled with the number of the methylene group

connecting two quaternary ammonium groups. Ion-association constants were determined by CE between the divalent quaternary ammonium ions and isomers of divalent aromatic anions such as naphthalene-2,6-disulfonate ion (2,6-NDS). Intramolecular distance between two anionic groups is fixed by the rigid structure of the aromatic anions. Ion-association constants are plotted against the intra-atomic distance between two ammonium sites (Fig. 7). The ion-associability of divalent naphthalenedisulfonate ions greatly increased from propane bis(triethylammonium) ion ($PrB(TEA)^{2+}$) to pentane bis(triethylammonium) ion ($PeB(TEA)^{2+}$). The result was interpreted with synergistic effects: increased hydrophobicity of the pairing cation and the fitting of the intra-ionic distance of the divalent cations to the divalent anions. On the other hand, the increase in the ion-associability was slight from $PeB(TEA)^{2+}$ to heptane bis(triethylammonium) ion ($HpB(TEA)^{2+}$). The result was attributed to the conflict of the two factors: the increase in the hydrophobicity of the pairing cation and the decrease in the distance fitting between the cation and the anion. The selectivity of the divalent quaternary ammonium ions changed with the positional isomers of the naphthalenedisulfonate ions. The selectivity also agreed with the distance fitting of the pairing ions between the divalent quaternary ammonium ions and the divalent aromatic anions [37].

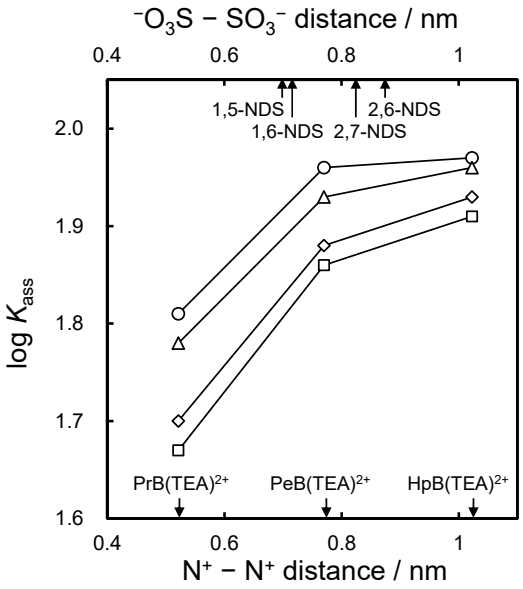

Fig. 7. Change in ion-association constant of anions associated with intra-atomic distance. NDS isomers: ○, 1,5-NDS; △, 1,6-NDS; □, 2,6-NDS; ◇, 2,7-NDS. Rearranged from a figure in Ref. 37.

Aromatic-aromatic interaction (π–π interaction) was examined between some polyaromatic cations and anions [38]. A polyaromatic cation was added in the separation buffer and the effective electrophoretic mobility of some polyaromatic anions was measured by CE. Logarithmic values of K_{ass} were also plotted against the total carbon number of the ion-associate, and contribution of the hydrophobicity was discussed (Fig. 8). Logarithmic value of K_{ass} increased about 0.14 by the increase in one unit of the carbon. Considering that 0.06 of the increment is contributed from the hydrophobicity of a methylene group or a carbon moiety, the difference, 0.08, is attributed to the contribution of the aromatic-aromatic interaction [38]. Aromatic-aromatic interaction was also revealed with divalent viologen cations [39].

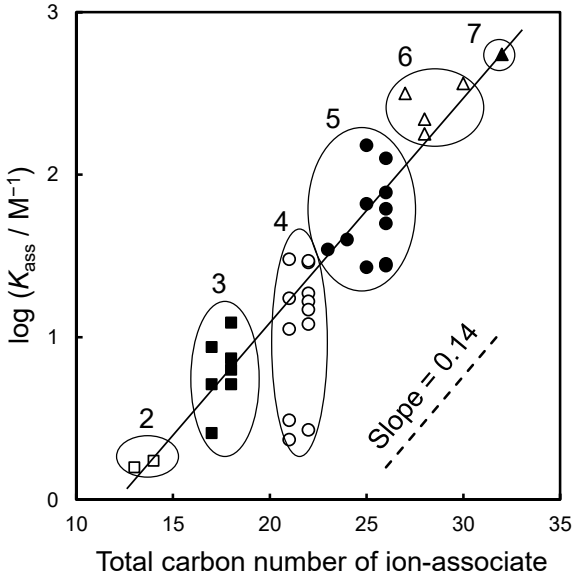

Fig. 8. Plots of log K_{ass} values against the total carbon number of ion-associate. Numbers in the figure indicate the total aromatic ring of ion-associates. Rearranged from a figure in Ref. 38.

Table 1. Intermolecular ion-ion interactions found to work in an aqueous solution

Interaction	Illustration	Detail
Electrostatic	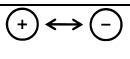	Highly charged ions are more associable.
Hydrophobic	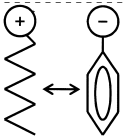	One methylene moiety contributes about $10^{0.06}$ to K_{ass}. The contribution is about 1/10 of the liquid-liquid distribution.
Multipoint	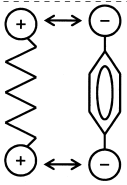	Distance between two ionic groups in a molecule is recognized.
π − π	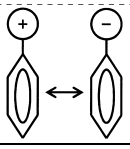	One carbon contributes about $10^{0.08}$ to K_{ass}, in addition to the hydrophobicity.

Partly cited from Ref. 1.

It is also mentioned that such CE analysis of the ion-association equilibrium is applicable to precipitable ion-associates because of the superb hydrophobicity [40]. Factors contributing to the ion-associability in an aqueous solution are summarized in Table 1 [1].

3.5. Application to the ion-pair solvent extraction

Clarification of the ion-association process in an aqueous solution leads to the understanding of the stepwise equilibria of ion-pair extraction. It is assumed in ion-pair extraction that an ion-associate $C^+ \cdot A^-$ is formed in an aqueous solution between a cation C^+ and an anion A^- and that the ion-associate formed is distributed to the organic phase as shown in Fig. 9.

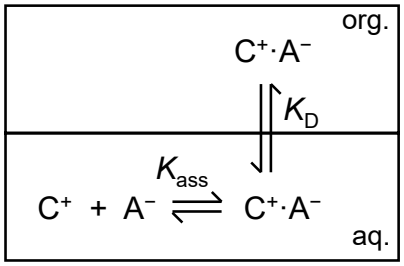

Fig. 9. Schematic illustration of ion-pair extraction and stepwise reactions.

An ion-pair extraction equilibrium is expressed as in Eq. (9), with an ion-pair extraction constant, K_{ex}, as in Eq. (10).

$$C^+ + A^- \overset{K_{ex}}{\rightleftharpoons} C^+ \cdot A^-_{(o)} \qquad (9)$$

$$K_{ex} = \frac{[C^+ \cdot A^-]_{(o)}}{[C^+][A^-]} \qquad (10)$$

In Eqs. (9) and (10), the subscript (o) denotes the species in the organic phase. The extraction equilibrium is divided into two stepwise equilibria: an association process in an aqueous solution as in Eq. (5) and a distribution process as in Eq. (11), with their equilibrium constants, Eqs. (6) and (12), respectively.

$$C^+ \cdot A^- \overset{K_D}{\rightleftharpoons} C^+ \cdot A^-_{(o)} \qquad (11)$$

$$K_D = \frac{[C^+ \cdot A^-]_{(o)}}{[C^+ \cdot A^-]} \qquad (12)$$

In Eqs. (11) and (12), K_D is a distribution coefficient of the ion-associate. It is noticed from Fig. 9 and equilibrium constants that the ion-pair extraction constant is a product of ion-association constant in an aqueous solution and distribution coefficient of the ion-associate, as in Eq. (13).

$$K_{ex} = K_{ass} \times K_D \qquad (13)$$

It had been difficult to determine the ion-association constants in an aqueous solution and to divide the contribution of the two stepwise reactions to the whole extraction constant [25]. However, the CE analysis realized the direct determination of the K_{ass} values in an aqueous solution, and the K_D value can be calculated by $K_D = K_{ex}/K_{ass}$. Thus, the contributions of the stepwise reactions were resolved [41]. It is noticed by the comparison between K_{ass} and K_D that distribution process is predominant in K_{ex} [41,42]. The contributions of K_{ass} and K_D to K_{ex} agree with the hydrophobic ion-ion interaction in an aqueous solution, about 1/10 of the liquid-liquid extraction [32].

The stepwise reactions in liquid-liquid extraction system were also examined with the solvent extraction of alkali metal ions with crown ethers [43]. Alkali metal complexes are cationic, and they are extracted into an organic phase with a hydrophobic anion as ion-associates as shown in Fig. 10. Ion-pair extraction constants, K_{ex}, have been determined through the extraction experiments. The ion-pair extraction process consists of four equilibria: (1) partition of a crown ether L between aqueous and organic phases ($K_{D,L}$), (2) formation of a hydrophobic complex ML^+ with the crown ether (K_{ML}), (3) formation of an ion-associate $ML^+ \cdot X^-$ in an aqueous solution with a hydrophobic anion X^- (K_{MLX}), and (4) partition of the ion-associate $ML^+ \cdot X^-$ to the organic phase ($K_{D,MLX}$). Distribution coefficient of a crown ether, $K_{D,L}$, can be determined by solvent extraction, and CE analysis can determine both the complex formation constant K_{ML} and the ion-association constant K_{MLX}. Therefore, $K_{D,MLX}$ has firstly been determined by directly determining K_{MLX} by CE [43-45].

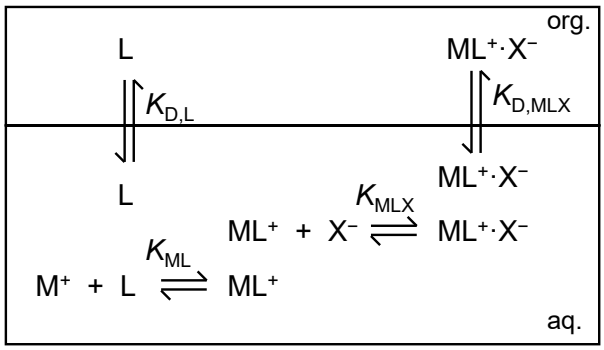

Fig. 10. Schematic illustration of ion-association extraction of crown ether complex of alkali metal ions.

4. Characterization of carbon nanoclusters by CE

4.1. Characterization of graphene and carbon nanotube

Since CE is operated in an open-tubular capillary without any solid-phase packing material, it is suitable for the characterization of carbon nanoclusters such as graphene and carbon nanotube with their size up to sub-micrometer

level. Graphene is a class of two-dimensional carbon material, and its physical properties of nano-sized sheets are standing in the center of attention [46]. Graphene, especially graphene oxide, was characterized by two CE studies [47,48]. Graphene easily aggregates in an aqueous solution by van der Waals interactions, and it has been recommended to use dilute ammonium acetate buffer to suppress the aggregation [47]. To avoid the aggregation of graphene, anionic charge has been given to electrically neutral graphene with dodecylbenzenesulfonate ion (DBS^-), and a CE separation of the negatively charged graphene has been made [49]. Since graphene does not possess unique structure but wide variety of size and shape, a broad peak has been obtained with graphene [49]. In the case of such surfactants as linear alkylsulfonates or alkyl sulfates, the number of shot signals, result of the aggregation, increased with the extension of the alkyl chain length, but a clear broad signal was not obtained with a triangular or Gaussian shape. Electropherograms of graphene are shown in Fig. 11 with varying concentrations of DBS^- in the separation buffer. Irreproducible shot signals emerged in the electropherograms at high concentrations of DBS^-. It would be because of the aggregation promoted by increased salt concentrations. When anionic charge was given to the graphene by $KMnO_4$ oxidation, the chemically modified graphene was resolved by CE from the graphene itself [49].

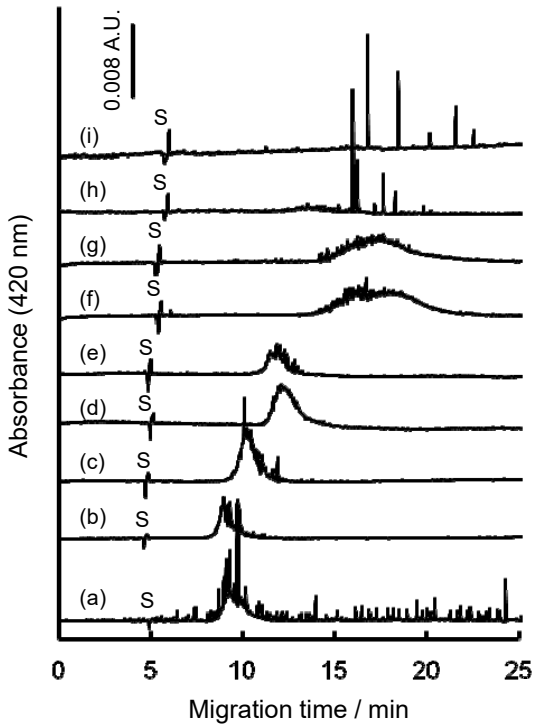

Fig. 11. Electropherograms of Graphene Nanoplatelets with varying concentrations of SDBS. Concentrations of SDBS (mmol dm^{-3}): (a) 6; (b) 7; (c) 15; (d) 20; (e) 25; (f) 35; (g) 40; (h) 45; (i) 50. Concentration of graphene, 2 mg/mL; S, electroosmotic flow. Cited from Ref. 49.

Polymer matrices of polyethylene glycol (PEG), poly(vinyl alcohol), and polyvinylpyrrolidone were also examined to develop the dispersion of graphene in an aqueous surfactant solution [50]. While the dispersion of graphene in an aqueous solution was developed with PEG, the effective electrophoretic mobility of the surfactant-adsorbed graphene decreased. The result suggested that the anionic surfactant on the graphene surface was competitively substituted with the nonionic polymer [50]. Poly(4-styrenesulfonate) ion (PSS) was also examined as a dispersion modifier [51]. PSS is an anionic polymer, and it irreversibly adsorbed graphene.

Carbon nanotube (CNT) is also a class of carbon nanoclusters, and it has been dispersed in an aqueous surfactant solution. The dispersion of CNT was analyzed by CE [52]. In contrast to the graphene dispersion, sodium dodecyl sulfate (SDS) worked well for the dispersion of CNT. While graphene is planar and it would interacts with benzene ring in DBS^-, CNT possesses a curved surface and SDS would be suitable for the adsorption to the CNT surface [52].

4.2. Characterization of carbon nanodots

Carbon nanodot (CND) is also classified as carbon nanoclusters, and it is attracting the most attentions in analytical and biomedical research with its less toxicity [53-55]. CE is found to be a useful technique to characterize and to utilize the CNDs. By using the CE characterization, cationic, less-charged and anionic CNDs were found in the CND prepared from citric acid and 1,2-ethylenediamine [56]. CND and CND-antibody bioconjugates were separated by CE [57].

Water-soluble carbon nanodots were prepared under microwave irradiation from glutamic acid or glutamic acid - boric acid mixture. The CNDs thus prepared were characterized by CE [58]. Typical electropherograms are shown in Fig. 12. A peak signal of anionic substance was detected in the electropherogram, and it was found to be a major component of the CNDs. The effective electrophoretic mobility of the major component was almost identical over the pH range between 6.7 and 11.6, suggesting that the functional group of amine or boric acid moiety was not included in the CNDs [58]. A signal of less-charged CNDs was also detected in the electropherogram, and the CNDs were characterized by a CE format of micellar electrokinetic chromatography. Two or four peaks were detected just after the electroosmotic flow; the less charged CNDs were thus hydrophilic [58]. Electric furnace was also used for the preparation of CNDs [59]. Glutamic acid or glutathione were used as a starting material of CND, and two major peaks of anionic and less-charged CNDs were also detected by CE with each of the CNDs.

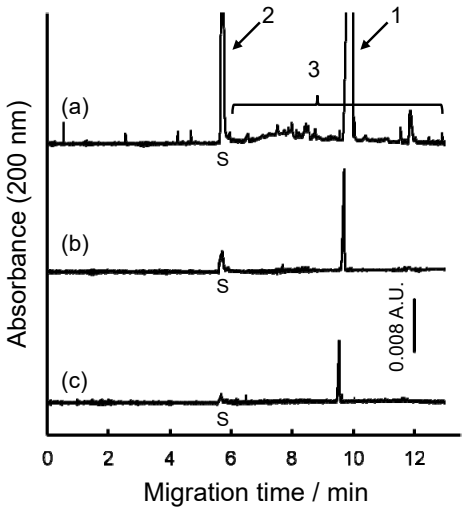

Fig. 12. Electropherograms of the BG-CND at different dilution factors. Dilution factor of the BG-CND solution: (a), 10 fold; (b), 100 fold; (c), 200 fold. Signals assigned are: 1, a major component of anionic CNDs; 2, less-charged component(s) of CNDs; 3, various minor components of anionic CNDs. S: solvent (EOF). Cited from Ref. 58.

5. Development of capillary electrophoresis/dynamic frontal analysis (CE/DFA)

5.1. Enzymatic reaction in a separation capillary

CE is widely used in the dynamic or kinetic reactions of enzymes. Enzymatic reaction is generally written as in Eq. (14). A substrate S forms a complex ES by an equilibrium reaction with an enzyme E, and a product P is kinetically generated from the complex; both an equilibrium and a kinetic reaction are involved. The equilibrium constant, K_M, is called as Michaelis-Menten constant and it is of great interest in enzymatic reactions.

$$\mathrm{E} + \mathrm{S} \underset{}{\overset{K_M}{\rightleftharpoons}} \mathrm{ES} \overset{k}{\rightarrow} \mathrm{P} \qquad (14)$$

The utilization of CE on enzyme assays is divided broadly into two categories. One is the pre-capillary reaction format and the other is an in-capillary reaction format. The latter is commonly called as electrophoretically mediated microanalysis (EMMA) [60-62]. In the pre-capillary format, the enzymatic reaction is done in a sample vial containing both an enzyme and a substrate. A small portion of the reaction solution is periodically analyzed, and the product is quantified by CE or micellar electrokinetic chromatography. Michaelis-Menten constants have been determined through the quantification results. CE format of an in-capillary reaction (EMMA) is more attractive on investigating the reaction dynamics of an enzyme. One of the first EMMA was reported with glucose-6-phosphate dehydrogenase [61]. Both an enzyme solution and a substrate solution, which contained a substrate of glucose-6-phosphate and a coenzyme of NADP, were tandemly injected into the capillary. When a DC voltage was applied to the capillary, the two zones electrophoretically counter-migrated in the capillary and a zone of the enzyme passed through the sample zone. In a period of the enzyme zone passing through the substrate zone, the enzymatic reaction proceeded and the products of 6-phosphogluconate and NADPH were constantly formed. A plateau signal of the formed NADPH was detected and used for the enzyme assay. While the plateau signal was instable at the early stage of the EMMAs, the stability of the plateau signal was developed by thermosetting [62]. Immobilized capillary enzyme reactor (IMER) [63] and transverse diffusion of laminar flow profiles (TDLFP) [64] have also reported as one of the formats of EMMA.

5.2. Michaelis-Menten analysis through CE/DFA

When a sample solution containing equilibrium species is introduced into a capillary with a relatively long plug, one of the equilibrium species, usually unbound (free) species of a small ion, electrophoretically migrates in the capillary and a long zone of the unbound species is detected as a plateau signal as a result of bound/free (B/F) separation. This format of CE is called as capillary electrophoresis/frontal analysis (CE/FA) [65]. The height of a plateau signal is used for quantification of the unbound species, and CE/FA has been utilized for equilibrium or affinity analysis [66,67].

A new mode of EMMA has been proposed as capillary electrophoresis/dynamic frontal analysis (CE/DFA) [68]. When a capillary is filled with an enzyme solution and a

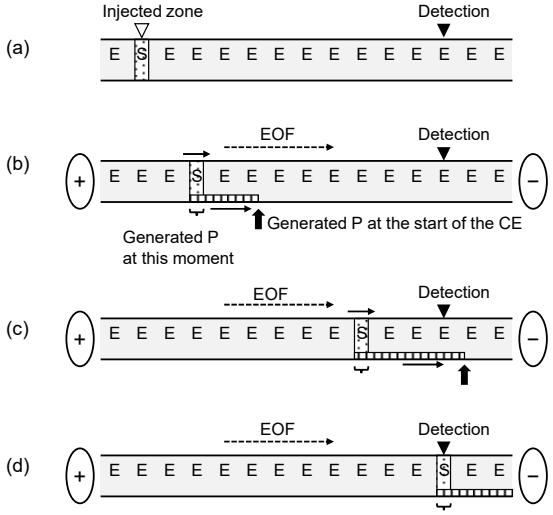

Fig. 13. Schematic illustration for the detection mechanism of CE/DFA. (a) A sample plug containing a substrate (S) is injected into a capillary. (b) A substrate electrophoretically migrates in the enzyme solution under applied DC voltage, where the substrate is continuously hydrolyzed to form a product (P). (c) Continuously generated product is detected, providing a plateau signal. (d) Finally, the residual substrate is detected at the end of the plateau signal. Rearranged from a figure in Ref. 68.

substrate solution is introduced into the capillary, a zone of the substrate would migrate in the separation buffer by electrophoresis. Enzymatic reaction proceeds at the substrate zone during the electrophoretic migration, and a reaction product would continuously be generated by the enzymatic reaction. When the electrophoretic mobility of the product is different from that of the substrate, the reaction product would continuously be resolved from the substrate zone. Since the reaction rate of the kinetic reaction is constant under sufficient concentrations of the substrate, the concentration of the resolved product would be kept constant. As a result of the constant reaction rate and the continuous CE resolution, a plateau signal would be detected with the product (Fig. 13) [68]. This plateau signal of the product is pulled out from the short zone of the substrate by the dynamic enzymatic reaction, and this format is comparable to CE/FA. While ordinary CE/FA is based on the separation of the equilibrium species from the equilibrium mixture, the EMMA-based plateau signal is a result of the dynamic reaction of an enzyme. Therefore, the EMMA format is called as CE/DFA.

Enzymatic hydrolysis of 4-nitrophenyl phosphate (NPP) with alkaline phosphatase (ALP) has been demonstrated as an example of CE/DFA [68]. 4-Nitrophenolate ion (NP) is generated from the substrate NPP by the enzymatic hydrolysis. Effective electrophoretic mobility of NP is smaller than that of NPP, and continuously generated NP is detected as a plateau signal prior to NPP (Fig. 14) Michaelis-Menten constant was determined through the

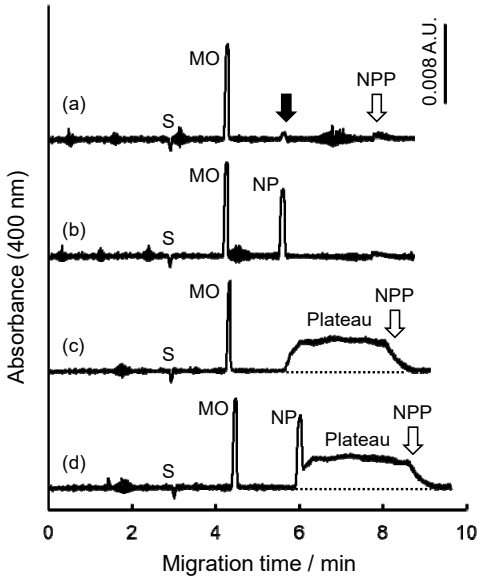

Fig. 14. Detection of a plateau signal of NP by the enzymatic reaction of NPP with ALP. (a) Detection of NPP without ALP. (b) Detection of NP without ALP. (c) Detection of NPP in the presence of ALP in the separation buffer. (d) Detection of NPP and NP in the presence of ALP in the separation buffer. MO: methyl orange as an internal standard. S: solvent (EOF). Cited from Ref. 68.

plateau height [68]. Because CE/DFA includes electrophoretic resolution of the product from the substrate zone, CE/DFA possesses such advantages that inhibition of enzymatic reactions by the reaction product is eliminated [68]. The enzymatic assay was also successful with carboxylesterase [69]. A pressure assist was utilized in the CE/DFA to detect the product zone fast and to average the fluctuated plateau signal by mixing in a laminar flow [69].

5.3. Inhibition analysis by CE/DFA

Analysis method of CE/DFA was applied to the inhibition assay of an enzyme [70]. When a substrate and an inhibitor are tandemly introduced into the capillary containing an enzyme in the separation buffer, inhibition of the enzymatic reaction occurs during the period of overlapping of the inhibitor zone to the substrate zone (Fig. 15). An inhibitor of theophylline was used on the enzymatic hydrolysis of 4-nitrophenyl phosphate with alkaline phosphatase. Two-steps of plateau signal was detected in the electropherogram. A higher plateau is based on the CE/DFA without inhibition, and a suppressed plateau is formed under the inhibition. Inhibition constant, as well as the Michaelis-Menten constant, was successfully determined through the plateau heights [70].

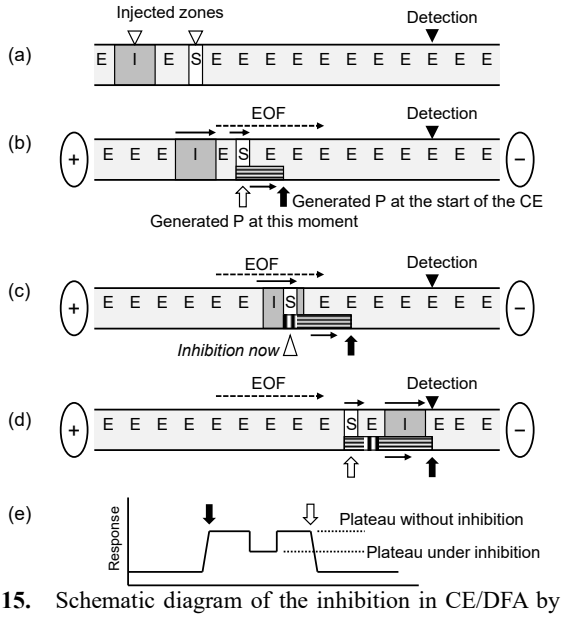

Fig. 15. Schematic diagram of the inhibition in CE/DFA by the tandem injections of a substrate and an inhibitor solutions (a) − (d), and a typical electropherogram (e). The inhibition occurs when the zones of a substrate (S) and an inhibitor (I) overlap by the electrophoretic migration. E: an enzyme contained in the separation buffer. Cited from Ref. 70.

5.4. Competition analysis by CE/DFA

Substrate competition is found in various biochemical processes [71]. In cases of one enzyme reacting with two substrates or two enzymes reacting with one substrate, such enzymatic activities are different from a single substrate

reaction, due to the competition. Substrate competition is comparable to the enzyme inhibition, because one of the substrates works as an inhibitor against another substrate [71].

Competitive inhibition between two substrates with an enzyme is investigated by CE/DFA [72]. Enzymatic hydrolyses of *o*-nitrophenyl *β*-D-galactopyranoside and *p*-nitrophenyl *β*-D-galactopyranoside with *β*-D-galactosidase were examined as a model competitive reaction. The reaction scheme is illustrated in Fig. 16. A sample solution containing the two substrates of S_1 and S_2 was injected into a capillary filled with a separation buffer containing an enzyme. Enzymatic hydrolysis occurred during the electrophoresis, and the products of P_1 and P_2 were continuously formed and resolved from the substrate zone. Two-steps plateau signal was detected with the two-substrate solutions based on the difference in the effective electrophoretic mobility of *o*-nitrophenol and *p*-nitrophenol as products. Michaelis-Menten constants and inhibition constants were determined with the plateau heights [72].

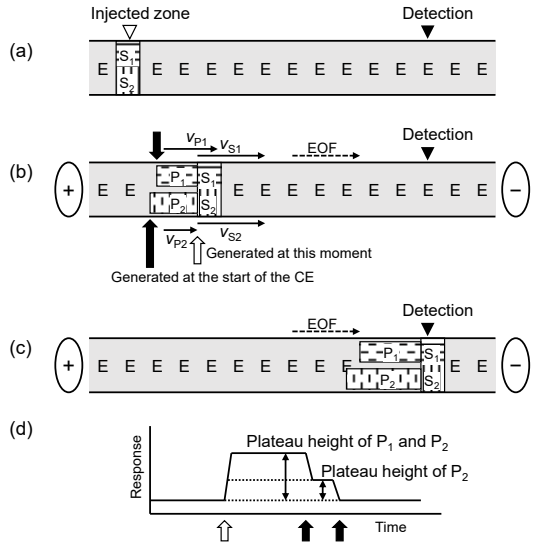

Fig. 16. Schematic migration diagram of two-substrates competitive reaction in CE/DFA. (a) – (c) Two products of P_1 and P_2 are formed from two substrates of S_1 and S_2 during the electrophoresis. An electropherogram (d) is expected by the competitive reaction; two products of P_1 and P_2 are detected as two-steps plateau signals by the enzymatic reaction. Cited from Ref. 72.

5.5. Analysis of reversible enzymatic reaction by CE/DFA

Enzymatic reaction with transferase directs the selective transfer of a substituent from one substrate to another substrate [73]. Transphosphorylation with creatine kinase (CK) is reversible between creatine (Cr) and creatine phosphate (CrP). Reverse reactions inevitably accompany in general batch analyses. Kinetic reactions of the transphosphorylation were individually investigated by pressure-assisted capillary electrophoresis/dynamic frontal analysis (pCE/DFA) [74]. In pCE/DFA, the kinetic reaction proceeds in a separation capillary, and the product is continuously resolved from the substrate zone. The formation rate is thus kept constant at the substrate zone without the reverse reaction, and the product is detected as a plateau signal. A plateau signal was detected in the pCE/DFA with ADP or ATP as one of the products on either the forward or the backward reactions as illustrated in Reaction (15).

$$\mathrm{Cr} + \mathrm{ATP} \underset{\mathrm{CK}}{\rightleftharpoons} \mathrm{CrP} + \mathrm{ADP} \qquad (15)$$

Michaelis-Menten constants of the forward and the backward reactions were successfully determined through the plateau signal without any interference from the reverse reaction [74].

6. Conclusion

With help of reaction dynamics in a separation capillary, capillary electrophoresis would be utilized on analyses of equilibrium and characterization of substances, in addition to practical quantifications and determinations. Effective electrophoretic mobility reflects the fractions of the analyte species of interest in fast equilibrium. The equilibrium would be analyzed through the effective electrophoretic mobility. Since electrophoretic resolution is involved in CE analysis, gradually generated substances, as well as coexisting impurities, are resolved from the equilibrium species, and equilibria of interest would be analyzed without interference from foreign substances. Dynamics in equilibrium and kinetics are often involved in labile substances, and kinetical phenomena would be also analyzed by coupling with CE separations as is CE/DFA.

Acknowledgements

The author would like to thank Emeritus professor Shoji Motomizu (Okayama University) for his fruitful suggestions. The author profoundly grateful to staffs, as well as graduate and undergraduate students in Okayama University and Tokushima University, who have worked on and promoted the research. In addition, the author thanks collaborators who have accomplished valuable research. A part of the study was financially supported by several KAKENHI projects from the Japan Society for the Promotion of Sciences (09740555, 19550090, 26410154, 17K05903, 20K05568).

References

[1] Takayanagi, T. *Anal. Sci.* **2004**, *20*, 255-265.
[2] Takayanagi, T. *Chromatography* **2005**, 26, 11-21.
[3] Poole, S. K.; Patel, S.; Dehring, K.; Workman, H.;

Poole, C. F. *J. Chromatogr. A* **2004**, *1037*, 445-454.
[4] Berezovski, M.; Krylov, S. N. *J. Am. Chem. Soc.* **2002**, *124*, 13674-13675.
[5] Krylov, S. N.; Berezovski, M. *Analyst* **2003**, *128*, 571-575.
[6] Krylov, S. N. *Electrophoresis* **2007**, *28*, 69-88.
[7] Kanoatov, M.; Galievsky, V. A.; Krylova, S. M.; Cherney, L. T.; Jankowski, H. K.; Krylov, S. N. *Anal. Chem.* **2015**, *87*, 3099-3106.
[8] Ishihama, Y.; Oda, Y.; Asakawa, N. *J. Pharm. Sci.* **1994**, *83*, 1500-1507.
[9] Tamura, Z.; Abe, S.; Ito, K.; Maeda, M. *Anal. Sci.* **1996**, *12*, 927-930.
[10] Takayanagi, T.; Motomizu, S. *Chem. Lett.* **2001**, *30*, 14-15.
[11] Örnskov, E.; Linusson, A.; Folestad, S. *J. Pharm. Biomed. Anal.* **2003**, *33*, 379-391.
[12] Simplício, A. L.; Gilmer, J. F.; Frankish, N.; Sheridan, H.; Walsh, J. J.; Clancy, J. M. *J. Chromatogr. A* **2004**, *1045*, 233-238.
[13] Tůma, P.; Samcová, E.; Balínová, P. *J. Chromatogr. B* **2005**, *821*, 53-59.
[14] Quesada-Molina, C.; García-Campaña, A. M.; del Olmo-Iruela, L.; del Olmo, M. *J. Chromatogr. A* **2007**, *1164*, 320-328.
[15] Nowak, P.; Olechowska, P.; Mitoraj, M.; Woźniakiewicz, M.; Kościelniak, P. *J. Pharm. Biomed. Anal.* **2015**, *112*, 89-97.
[16] Takayanagi, T.; Tabara, A.; Kaneta, T. *Anal. Sci.* **2013**, *29*, 547-552.
[17] Shimakami, N.; Yabutani, T.; Takayanagi, T. *Bunseki Kagaku* **2014**, *63*, 643-648.
[18] Takayanagi, T.; Amiya, M.; Shimakami, N.; Yabutani, T. *Anal. Sci.* **2015**, *31*, 1193-1196.
[19] Takayanagi, T.; Shimakami, N.; Kurashina, M.; Mizuguchi, H.; Yabutani, T. *Anal. Sci.* **2016**, *32*, 1327-1332.
[20] Itoh, D.; Mizuguchi, H.; Takayanagi, T. *Bunseki Kagaku* **2019**, *68*, 871-876.
[21] Tanikami, Y. Mizuguchi, H. Takayanagi, T. *Chromatography* **2021**, *42*, 49-54.
[22] Tanikami, Y.; Tagami, T.; Sakamoto, M.; Arakawa, Y.; Mizuguchi, H.; Imada, Y.; Takayanagi, T. *Electrophoresis* **2020**, *41*, 1316-1325.
[23] Takayanagi, T.; Itoh, D.; Mizuguchi, H. *Chromatography* **2016**, *37*, 105-109.
[24] Takayanagi, T.; Isoda, M.; Itoh, D.; Mizuguchi, H. *Bunseki Kagaku* **2017**, *66*, 509-514.
[25] Motomizu, S. *Bunseki Kagaku* **1999**, *48*, 151-181.
[26] Motomizu, S.; Tôei, K.; Iwachido, T. *Bull. Chem. Soc. Jpn.* **1969**, *42*, 1006-1010.
[27] Nashabeh, W.; Rassi, Z. E. *J. Chromatogr. A* **1991**, *536*, 31-42.
[28] Iki, N.; Hoshino, H.; Yotsuyanagi, T. *J. Chromatogr. A* **1993**, *652*, 539-546.
[29] Gotti, R.; Andrisano, V.; Cavrini, V.; Bertucci, C.; Furlanetto, S. *J. Pharm. Biomed. Anal.* **2000**, *22*, 423-431.
[30] Shelton, C. M.; Koch, J. T.; Desai, N.; Wheeler, J. F. *J. Chromatogr. A* **1997**, *792*, 455-462.
[31] Takayanagi, T.; Motomizu, S. *Chem. Lett.* **1995**, *24*, 593-594.
[32] Takayanagi, T.; Wada, E.; Motomizu, S. *Analyst* **1997**, *122*, 57-62.
[33] Takayanagi, T.; Tanaka, H.; Motomizu, S. *Anal. Sci.* **1997**, *13*, 11-18.
[34] Takayanagi, T.; Ban, N.; Takao, H.; Nakamura, N.; Oshima, M.; Motomizu, S. *Anal. Sci.* **1999**, *15*, 593-596.
[35] Rasmussen, B. W.; Bjerrum, M. J. *J. Chromatogr. A* **1999**, *836*, 93-105.
[36] Takayanagi, T.; Wada, E.; Oshima, M.; Motomizu, S. *Bull. Chem. Soc. Jpn.* **1999**, *72*, 1785-1791.
[37] Takayanagi, T.; Wada, E.; Motomizu, S. *Analyst* **1997**, *122*, 1387-1391.
[38] Takayanagi, T.; Ban, N.; Wada, E.; Oshima, M.; Motomizu, S. *Bull. Chem. Soc. Jpn.* **2000**, *73*, 669-673.
[39] Wada, E.; Takayanagi, T.; Motomizu, S. *Analyst* **1998** *123*, 493-495.
[40] Takayanagi, T.; Ogura, K.; Yabutani, T. *Anal. Sci.* **2014**, *30*, 919-924.
[41] Motomizu, S.; Takayanagi, T. *J. Chromatogr. A* **1999**, *853*, 63-69.
[42] Takayanagi, T.; Wada, E.; Motomizu, S. *Bunseki Kagaku* **1997**, *46*, 467-475.
[43] Takayanagi, T.; Iwachido, T.; Motomizu, S. *Bull. Chem. Soc. Jpn.* **1998**, *71*, 1373-1379.
[44] Manege, L. C.; Takayanagi, T.; Oshima, M.; Motomizu, S. *Analyst* **2000**, *125*, 699-703.
[45] Manege, L. C.; Takayanagi, T.; Oshima, M.; Motomizu, S. *Analyst* **2000**, *125*, 1928-1932.
[46] Geim, A. K.; Novoselov, K. S. *Nat. Mater.* **2007**, *6*, 183-191.
[47] Müller, M. B.; Quirino, J. P.; Nesterenko, P. N.; Haddad, P. R.; Gambhir, S.; Li, D.; Wallace, G. G. *J. Chromatogr. A* **2010**, *1217*, 7593-7597.
[48] Zhao, J.; Chen, G.; Zhang, W.; Li, P.; Wang, L.; Yue, Q.; Wang, H.; Dong, R.; Yan, X.; Liu, J. *Anal. Chem.* **2011**, *83*, 9100-9106.
[49] Takayanagi, T.; Morimoto, M.; Yabutani, T. *Anal. Sci.* **2013**, *29*, 769-771.
[50] Takayanagi, T.; Becchaku, Y.; Tomiyama, Y.; Kurashina, M.; Mizuguchi, H. *Anal. Sci.* **2019**, *35*, 307-313.
[51] Takayanagi, T.; Mizuta, Y.; Becchaku, Y.; Mizuguchi,

H. *Chromatography* **2019**, *40*, 121-126.
[52] Takayanagi, T.; Ikeuchi, K.; Mizuguchi, H. *Chromatography* **2017**, *38*, 101-106.
[53] Xu, X.; Ray, R.; Gu, Y.; Ploehn, H. J.; Gearheart, L.; Raker, K.; Scrivens, W. A. *J. Am. Chem. Soc.* **2004**, *126*, 12736-12737.
[54] Baker, S. N.; Baker, G. A. *Angew. Chem. Int. Ed.* **2010**, *49*, 6726-6744.
[55] Hu, Q.; Gong, X.; Liu, L.; Choi, M. M. F. *J. Nanomater.* **2017**, 1804178.
[56] Hu, Q.; Paau, M. C.; Zhang, Y.; Chan, W.; Gong, X.; Zhang, L.; Choi, M. M. F. *J. Chromatogr. A* **2013**, *1304*, 234-240.
[57] Wu, Y.; Remcho, V. T. *Talanta* **2016**, *161*, 854-859.
[58] Takayanagi, T.; Iwasaki, S.; Becchaku, Y.; Yabe, S.; Morita, K.; Mizuguchi, H.; Hirayama, N. *Anal. Sci.* **2020**, *36*, 941-946.
[59] Takayanagi, T.; Iwasaki, S.; Morita, K.; Hirayama, N.; Mizuguchi, H. *Chromatography* **2020**, *41*, 103-107.
[60] Scriba, G. K. E.; Belal, F. *Chromatographia* **2015**, *78*, 947-970.
[61] Bao, J.; Regnier, F. E. *J. Chromatogr. A* **1992**, *608*, 217-224.
[62] Whisnant, A. R.; Gilman, S. D. *Anal. Biochem.* **2002**, *307*, 226-234.
[63] Iqbal, J. *Anal. Biochem.* **2011**, *414*, 226-231.
[64] Krylova, S. M.; Okhonin, V.; Krylov, S. N. *J. Sep. Sci.* **2009**, *32*, 742-756.
[65] Gao, J. Y.; Dubin, P. L.; Muhoberac, B. B. *Anal. Chem.* **1997**, *69*, 2945-2951.
[66] Wiedmer S. K.; Lokajová, J. *J. Sep. Sci.* **2013**, *36*, 37-51.
[67] Štěpánová, S.; Kašička, V. *J. Sep. Sci.* **2015**, *38*, 2708-2721.
[68] Takayanagi, T.; Mine, M.; Mizuguchi, H. *Anal. Sci.* **2020**, *36*, 829-834.
[69] Mine, M.; Matsumoto, N.; Mizuguchi, H.; Takayanagi, T. *Anal. Methods* **2020**, *12*, 5846-5851.
[70] Mine, M.; Mizuguchi, H.; Takayanagi, T. *Chem. Lett.* **2020**, *49*, 681-684.
[71] Schäuble, S.; Stavrum, A. K.; Puntervoll, P.; Schuster, S.; Heiland, I. *FEBS Lett.* **2013**, *587*, 2818-2824.
[72] Mine, M.; Mizuguchi, H. Takayanagi, T. *J. Pharm. Biomed. Anal.* **2020**, *188*, 113390.
[73] Faber, K. *Biotransformations in Organic Chemistry. 5th ed.* Springer, Berlin, **2004**, pp. 123-134.
[74] Mine, M.; Mizuguchi, H.; Takayanagi, T. *Anal. Bioanal. Chem.* **2021**, *413*, 1453-1460.